

# CHARACTERIZATION OF MEMS MICROPHONE SENSITIVITY AND PHASE DISTRIBUTIONS WITH APPLICATIONS IN ARRAY PROCESSING

Patrick W.A. Wijnings<sup>\*†</sup>    Sander Stuijk<sup>\*</sup>    Rick Scholte<sup>†</sup>    Henk Corporaal<sup>\*</sup>

<sup>\*</sup> Eindhoven University of Technology, Eindhoven, The Netherlands

<sup>†</sup> Sorama, Eindhoven, The Netherlands

An array with MEMS microphones can distinguish individual noise sources in an environment through spatial filtering. Its effectiveness depends on the variations in microphone sensitivity and phase. Quantification of these variations is valuable, because it enables assessment and optimization of array performance. This is particularly important if the measurements are to be used for enforcement of noise regulations.

Nominal microphone sensitivity and phase are manufacturer-specified, but the distribution (histogram) around these values is not. Hence, this work demonstrates a free-field comparison method for measuring these variations in a batch of arrays. We also provide the histograms at 1 kHz for a sample population of 8384 Knowles SPH0641LM4H-1 MEMS microphones (131 arrays of 64 microphones). The histograms follow t-distributions, resulting in 95% confidence intervals of  $\pm 0.39$  dB for sensitivity and  $\pm 0.82^\circ$  for phase. Finally, we illustrate that delay-and-sum beamforming with these microphones results in a Gumbel-distributed gain with  $-0.13/+0.10$  dB 95% confidence interval.

**Index Terms**— Microphone arrays, Calibration, Array signal processing

## 1. INTRODUCTION

Excessive noise is harmful for human health and can disturb sleep and cause psychophysiological and cardiovascular effects [1]. According to the World Health Organization, one in five Europeans is regularly exposed to sound levels at night that could significantly damage health [1]. To this end, governments limit noise pollution through noise regulations [2].

Enforcement of these regulations requires reliable acoustic measurements. These are usually recorded using sound pressure level (SPL) meters whose requirements are defined in the *International Electrotechnical Commission (IEC) 61672* standard [3].

However, SPL meters cannot separate the contribution of each individual source to the overall SPL which is desirable when there are multiple noise sources in an environment. In contrast, arrays of multiple microphones in combination with spatial filtering algorithms such as beamforming [4, 5] are specifically tailored for this task. Such arrays are commercially available (e.g. from *Sorama, Fluke, Norsonic, gfai tech, CAE systems, FLIR Systems*) and typically have 32–128 microphones, with *Sorama* holding the Guinness world record for the largest microphone array consisting of 4096 microphones [6].

Array processing fuses the measurements of many microphones. Hence, its effectiveness depends on the variations in microphone

sensitivity and phase [7] that occur due to the microphones' fabrication process [8]. Information about the extent of these microphone variations is valuable, because it enables quantification of the array performance, e.g. localization and SPL measurement uncertainty. This is particularly important if the measurements have legal implications. Also, if the distribution of the variations is known, the processing algorithm can be tuned to achieve better performance (e.g. minimum variance beamforming [4, Sec. IV]).

While SPL meters typically rely on analog condenser microphones due to their precision, stability and reliability [9], digital microphones based on *micro-electro-mechanical systems (MEMS)* technology [10] are more suitable for application in arrays, due to their significantly lower cost and small surface-mounted footprint which allows for robotized assembly of the microphones on printed circuit boards (PCBs). A MEMS microphone manufacturer commonly specifies a sensitivity tolerance at 1 kHz (typ.  $\pm 1$  dB [11]), and less commonly a phase tolerance at 1 kHz (typ.  $\pm 10^\circ$  [12]) and sensitivity tolerance for other frequencies (typ. up to  $\pm 3$  dB [13, Fig. 5]). However, the distributions (histograms) of the variations are uncommonly specified.

Hence, this work demonstrates a free-field comparison method for measuring the sensitivity and phase distributions of a batch of MEMS microphone arrays (Sec. 2). This method is of interest to people who want to determine microphone attributes not specified by their supplier. We also provide the sensitivity and phase offsets at a frequency of 1 kHz for a sample population of 8384 MEMS microphones (131 arrays of 64 microphones) (Sec. 3). These empirical results are of interest to people who want to quantify (or optimize) performance of their array processing algorithms. In Sec. 4 we illustrate this on a delay-and-sum beamforming algorithm. Finally, we conclude this work in Sec. 5. In the spirit of open science, the data and scripts necessary to reproduce this work are provided online<sup>1</sup>.

## 2. MEASUREMENT METHOD

### 2.1. Measurement procedure

To determine the sensitivity and phase of the microphones, we used a free-field comparison method. Two arrays are placed in a measurement setup (Fig. 1) at 1 m distance from an acoustic source such that their microphones form adjacent pairs which approximately measure the same physical quantity, since the spacing between them ( $1.25 \pm 0.75$  mm) is small compared to the wavelength (34 cm for 1 kHz) and local extrema in the acoustic field due to standing waves are inhibited by absorption materials on the walls of the room (free-field condition). By comparing the measurements of each microphone pair, their differential sensitivity and phase can be determined.

This work is funded by the NWO Perspectief program ZERO.  
Correspondence to: p.w.a.wijnings@tue.nl.

<sup>1</sup><https://github.com/DutchRPW/ICASSP2021-microphone-calibration>

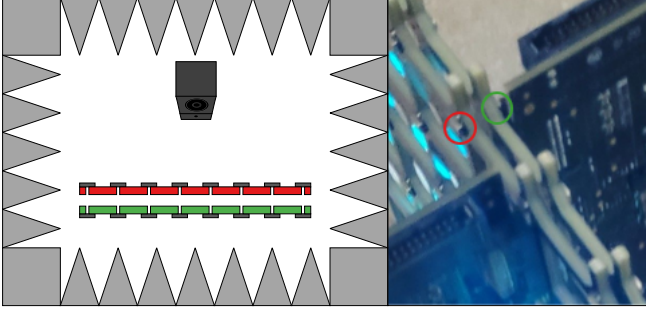


**Fig. 1:** Our measurement setup. The colored circles mark a pair of adjacent microphones (**device under test**, **reference**). The acoustic ports of the omnidirectional microphones are located on the bottom of the microphone packages, between the PCBs.

The key property of this method is that the differentials are insensitive to changes in the sound pressure level common to the pair of microphones. This greatly relaxes the constraints on temporal stability and spatial uniformity of the acoustic field. The price to pay for this is that the absolute sensitivity and phase are difficult to determine in this way. We deem this an acceptable trade-off, since the sensitivity and phase distributions can still be completely determined by augmenting our method with the nominal values available from the manufacturer’s specification.

To be able to recover the sensitivity and phase deviations of the *two* microphones from their *single* differential, we fixed one of the two arrays in the setup – the *reference* – while the other one was swapped after each measurement – the *device under test* (DUT). Since the properties of the microphone are deemed to remain stable over the duration of the measurement session, the sensitivity and phase of each reference microphone were recovered by computing the median of its differentials over the batch of DUTs. Then, the properties of each DUT microphone followed simply by subtracting the reference values from its differential.

Hence, this method has the advantage of not requiring access to a plurality of calibrated laboratory-grade reference microphones, as long as the batch is sufficiently large.

## 2.2. Equipment

The experiments were performed over a period of two days in the pseudo-anechoic room of Sorama’s acoustic laboratory in Eindhoven, The Netherlands. The room is not fully anechoic, but the walls and ceiling are covered with sound absorbing materials which reduce environmental noise as well as reflections inside the room.

For the microphone arrays, we used 156 bare Sorama CAM64 [14] array PCBs. One was randomly selected as the reference and the remaining 155 were used as DUTs. Each array contains 64 *Knowles SPH0641LM4H-1* (Morello) bottom-port MEMS microphones [11] in a uniform  $8 \times 8$  grid with 2 cm spacing. The PCBs contain cut-out slots between the microphones to make them as acoustically transparent as possible. A custom holder was 3D-printed to fix the spacing between the DUT and the reference.

For the acoustic source, an *Ultimate Ears MEGABOOM* bluetooth speaker was placed at 1 m distance from the DUT. The speaker was playing back a 1 kHz sine wave at  $68 \pm 9$  dB(SPL) (averaged over the DUT and reference arrays). Our results do not critically depend on this SPL, since it was well above the noise floor ( $\leq 32$  dB(SPL)) but below the acoustic overload point of the microphones (120 dB(SPL)).

Two *Sorama DMAIO* 64-channel Ethernet I/O interfaces were used to acquire 10 seconds of audio with 46875 Hz sample rate for resp. the DUT and the reference array. The boards were synchronized up to  $1 \mu\text{s}$  using the IEEE 1588 precision time protocol [15].

## 2.3. Data processing

Of the 155 recordings, 24 were discarded because they did not contain a usable signal due to issues with a connector and the acoustic source. The remaining recordings were processed with a discrete Fourier transform (DFT) with amplitude-corrected flat top window [16, Pg. 19], after which the 1 kHz frequency bin was extracted for each microphone channel. Dividing the complex number of each DUT microphone by its corresponding reference resulted in  $131 \times 64$  complex differential pairs, of which the *magnitude* (in decibel) corresponded to differential sensitivity and the *argument* (in degrees), corresponded to differential phase. Finally, the DUTs’ sensitivity and phase offsets from nominal were recovered from the differentials by – separately for each of the two measurement days – subtracting resp. the median sensitivity and phase over all the recordings for that reference microphone. We have visualized the resulting dataset in Fig. 2a–b.

## 2.4. Related work

Industry standard calibration methods are prescribed by IEC 60942 [17] and IEC 61094 [18]. At 1 kHz, an accuracy of about  $\pm 0.1$  dB (95% confidence interval) for sensitivity [19, Tbl. 1–4] and  $\pm 0.02^\circ$  (95% confidence interval) for phase [19, Tbl. 5] is achievable. However, since these methods are designed for condenser microphones, modifications are required for application on MEMS microphones due to their different form factor. Such modifications are reported by *Prato et al.* [20], who adapted the IEC 61094-5 free-field comparison method ( $\pm 0.37$  dB at 1 kHz, 95% confidence interval), and by *Wagner and Fick* [21], who adapted the IEC 61094-2 pressure reciprocity technique ( $\pm 0.12$  dB at 1 kHz, 95% confidence interval). Also, *Zuckerwar et al.* [22] report a substitution method for frequencies up to 80 kHz with uncertainty of  $\pm 0.41$  dB (68% confidence interval). While their reported accuracies for sensitivity are inspiring, they do not report results on phase. Also, their work does not teach how to generalize to calibration of arrays.

*Havránek et al.* [23] do present a free-field comparison method for calibrating array sensitivity and phase. However, while their measurement setup is similar to ours, their work focuses on the design of an acoustical source with predictable geometric field.

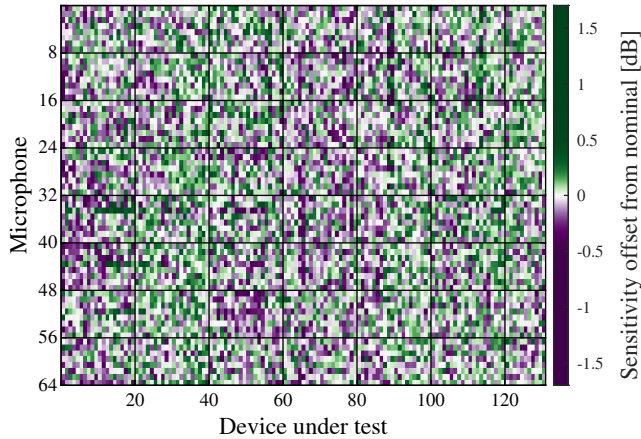
The focus of all above work is on calibration of *specific* sample devices, while ours is on determining the distributions of a *batch* of devices *around* the nominal sensitivity and phase. Hence, we can relax many constraints related to the reference microphones.

## 3. SENSITIVITY AND PHASE DISTRIBUTIONS

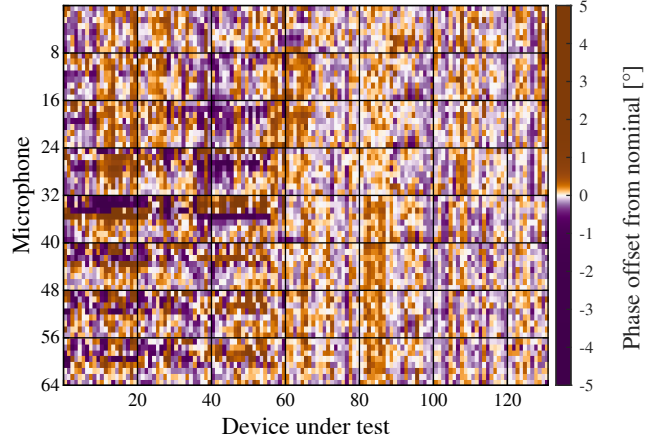
To recover the sensitivity and phase distributions, we aggregated the dataset (as visualized in Fig. 2a–b) into two histograms (Fig. 2c–d). The histograms closely follow a t-distribution:

$$p(x) = \frac{\Gamma(\frac{\nu+1}{2})}{\sigma\sqrt{\nu\pi}\Gamma(\frac{\nu}{2})} \left[ \frac{\nu + \left(\frac{x-\mu}{\sigma}\right)^2}{\nu} \right]^{-\left(\frac{\nu+1}{2}\right)}, \quad (1)$$

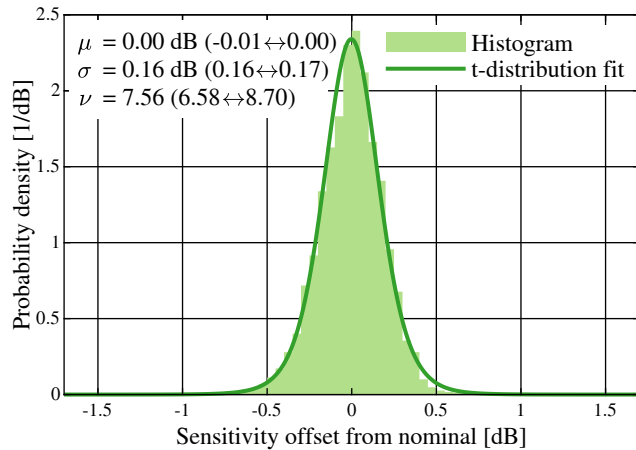
where  $\Gamma(\cdot)$  is the gamma function and  $\mu$ ,  $\sigma$  and  $\nu$  are parameters. The maximum-likelihood fits are also shown in Fig. 2c–d, from



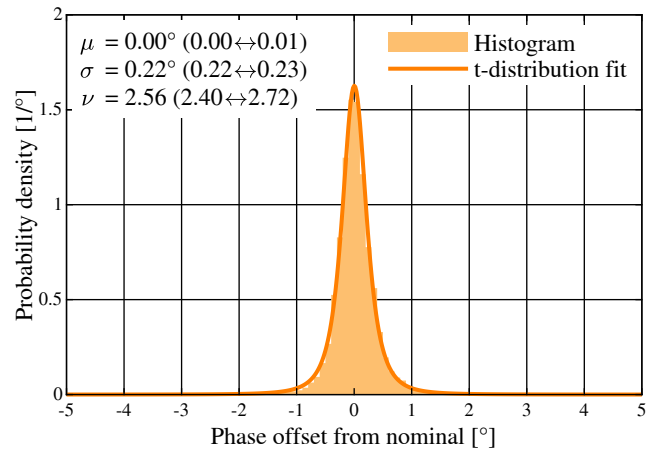
(a) Sensitivity offsets for all devices under test.



(b) Phase offsets for all devices under test.



(c) Distribution of sensitivity offset. Histogram bin width is 0.05 dB. The parameter values of the maximum-likelihood t-distribution fit are also shown, with 95% confidence intervals between parentheses.



(d) Distribution of phase offset. Histogram bin width is 0.1°. The parameter values of the maximum-likelihood t-distribution fit are also shown, with 95% confidence intervals between parentheses.

**Fig. 2:** Distribution of sensitivity and phase.

which we infer 95% confidence intervals of  $\pm 0.39$  dB for sensitivity and  $\pm 0.82^\circ$  for phase. The largest absolute offsets in the sample population are 1.68 dB for sensitivity and  $5.00^\circ$  for phase.

Because the maximum-likelihood values of  $\nu$  are rather small, the t-distribution provides a better fit than the normal distribution (which is equal to a t-distribution with  $\nu \rightarrow \infty$ ). Nonetheless, the t-distribution should still be considered an approximation for the underlying physics of the microphone. Hence, we report non-integer values for  $\nu$  [24].

By comparing the sensitivity results with the manufacturer's specification of  $\pm 1.00$  dB (100% tested) [11], we make two observations.

Firstly, due to the fat tail of the t-distribution, the specification is necessarily conservative to retain good production yields, i.e. the vast majority of the microphones fall inside the manufacturer's specification by a large margin.

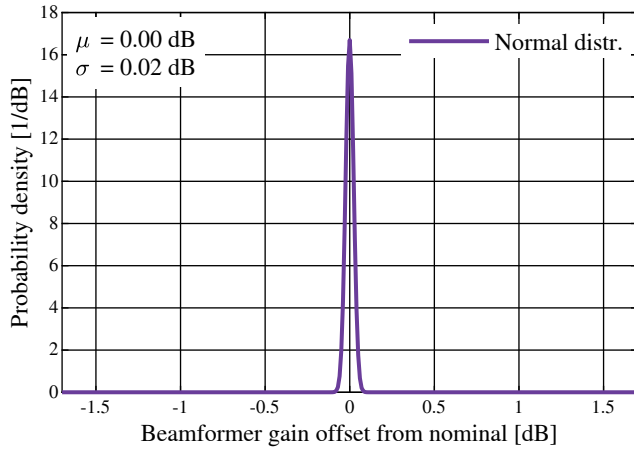
Secondly, of the 8384 measurements, ten data points fall outside the specification. This indicates that above distributions are likely over-estimated due to the tolerances in our measurement setup. For

example, the  $\pm 0.75$  mm tolerance in the spacing between the arrays causes a sensitivity variation of  $\pm 0.07$  dB due to the inverse square law, and a phase variation of  $\pm 0.79^\circ$  due to propagation delay. These variations appear as vertical streaks in Fig. 2a–b.

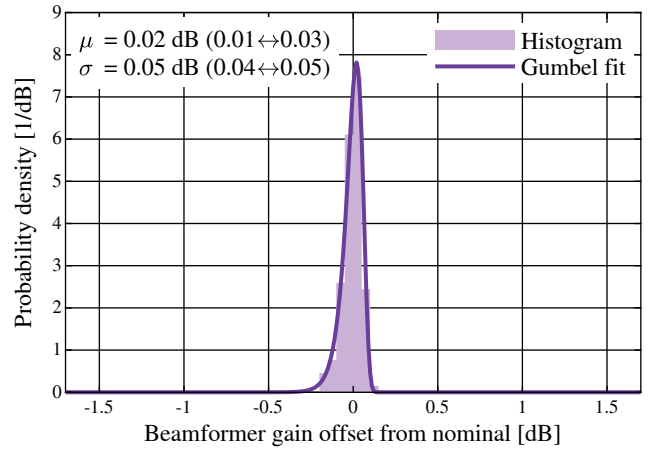
Nonetheless, our  $\pm 0.39$  dB confidence interval of the spread of an *uncalibrated* MEMS microphone is in the same range as the  $\pm 0.12$ – $0.82$  dB 95% confidence intervals of the calibration methods from the literature as discussed in Sec. 2.4. This suggests that, while calibration of MEMS microphones is useful for identifying *systematic* offsets from the manufacturer's nominal sensitivity, it has limited benefits for reducing random variations in the frequency range around 1 kHz.

#### 4. APPLICATION: ARRAY PERFORMANCE

To assess performance of an array's microphones working in unison, we consider the delay-and-sum beamforming algorithm. A beamformer combines the signals of all microphones in the array so that



(a) Based on maximum-likelihood t-distributions from Fig. 2c–d. The parameter values of the normal distribution are also shown.



(b) Based on sample population. Histogram bin width is 0.05 dB. The parameter values of the maximum-likelihood Gumbel distribution fit are also shown, with 95% confidence intervals between parentheses.

**Fig. 3:** Distribution of beamformer gain.

contributions from sources at particular angles experience constructive interference while others experience destructive interference. For a far-field source located on the broadside (i.e. perpendicular to the array), the gain of the delay-and-sum beamformer is given by:

$$G = 20 \log_{10} \left| \frac{1}{N} \sum_{n=1}^N w_n \cdot g_n \right|, \quad (2)$$

$$g_n \stackrel{\text{def}}{=} 10^{s_n/20} \cdot \exp\left(\frac{i\pi}{180} \varphi_n\right), \quad (3)$$

where  $G$  [dB] is the gain of the beamformer,  $N = 64$  is the number of microphones,  $w_n$  is the  $n$ th complex steering coefficient and  $g_n$  is the complex gain of the  $n$ th microphone. The sensitivity and phase offsets  $s_n$  [dB] and  $\varphi_n$  [°] correspond to Fig. 2. When the beamformer is looking into the same direction as above source, all  $w_n = 1$ . In that case the nominal output of the beamformer is unity, which corresponds to  $G = 0$  dB.

Firstly, we compute the distribution of  $G$  which would arise if the microphone offsets would be independently and identically distributed according to the maximum-likelihood t-distributions found in Sec. 3. The resulting distribution does not have a convenient mathematical form, but it can be closely approximated by a normal distribution:

$$p(G) = \frac{1}{\sigma\sqrt{2\pi}} \exp\left(-\frac{(G-\mu)^2}{2\sigma^2}\right), \quad (4)$$

where  $\mu$  and  $\sigma$  are parameters. The result is shown in Fig. 3a. The corresponding 95% confidence interval is  $\pm 0.05$  dB.

Secondly, we compute a histogram of 131 beamformer gains corresponding to the measured arrays. We do this to assess possible intra-array correlations. This histogram closely follows a Gumbel distribution:

$$p(G) = \sigma^{-1} \exp\left(\frac{G-\mu}{\sigma}\right) \exp\left(-\exp\left(\frac{G-\mu}{\sigma}\right)\right), \quad (5)$$

where  $\mu$  and  $\sigma$  are parameters. The histogram and the fit are shown in Fig. 3b. The corresponding (asymmetric) 95% confidence interval is  $-0.13/+0.10$  dB. The largest absolute offset in the sample population is 0.17 dB.

The discrepancy between both approaches shows that the measured offsets are slightly correlated within each array. Since this correlation is also clearly visible as vertical lines in Fig. 2a–b, we assess limitations of the measurement setup are a likely contributor, as previously discussed in Sec. 3.

## 5. CONCLUSION

We have demonstrated a free-field comparison method for measuring the sensitivity and phase deviations of a batch of MEMS microphone arrays. While the method has some limitations with respect to determination of absolute microphone parameters and measurement uncertainty, we have successfully applied it to show that the microphone deviations at 1 kHz can be modeled with t-distributions. The spread in sensitivity of the population of uncalibrated microphones is comparable with the uncertainty of a calibrated microphone as reported in the literature.

Using delay-and-sum beamforming, we also illustrated that array processing can further reduce this spread. The reduction is limited by intra-array correlations, although we assess that limitations of the measurement method are a likely contributor for these correlations.

Future work includes generalization to other frequencies in the audible and ultrasonic range, as well as assessment of long-term stability of the microphone parameters due to environmental influences.

## 6. ACKNOWLEDGMENTS

We would like to thank Vishnu Kannan, Achiel Schuurmans and Ivo Jansen, all employed at Sorama, for their help with performing the measurements.

## 7. REFERENCES

- [1] World Health Organization, *Burden of disease from environmental noise: quantification of healthy life years lost in Europe*, World Health Organization, Regional Office for Europe, Copenhagen, 2011, OCLC: 779684347.
- [2] World Health Organization, *Environmental noise guidelines for the European Region*, 2018, OCLC: 1129816077.
- [3] International Electrotechnical Commission, “IEC 61672-1/2/3, Electroacoustics - Sound level meters,” 2013.
- [4] B. D. van Veen and K. M. Buckley, “Beamforming: a versatile approach to spatial filtering,” *IEEE ASSP Magazine*, vol. 5, no. 2, pp. 4–24, Apr. 1988.
- [5] Patrick W.A. Wijnings, Sander Stuijk, Bert de Vries, and Henk Corporaal, “Robust Bayesian Beamforming for Sources at Different Distances with Applications in Urban Monitoring,” in *ICASSP 2019 - 2019 IEEE International Conference on Acoustics, Speech and Signal Processing (ICASSP)*, May 2019, pp. 4325–4329, ISSN: 2379-190X, 1520-6149.
- [6] Guinness World Records, “Largest microphone array,” <https://www.guinnessworldrecords.com/world-records/largest-microphone-array/> [Accessed: 18 September 2020].
- [7] Ivan Tashev, “Beamformer sensitivity to microphone manufacturing tolerances,” 2005.
- [8] S. Walser, C. Siegel, M. Winter, G. Feiertag, M. Loibl, and A. Leidl, “MEMS microphones with narrow sensitivity distribution,” *Sensors and Actuators A: Physical*, vol. 247, pp. 663–670, Aug. 2016.
- [9] Brüel & Kjær, “What Is A Sound Level Meter?,” <https://www.bksv.com/en/Knowledge-center/blog/BlogArticles/Sound-Measurement/what-is-a-sound-level-meter> [Accessed: 17 September 2020].
- [10] Siti Aisyah Zawawi, Azrul Azlan Hamzah, Burhanuddin Yeop Majlis, and Faisal Mohd-Yasin, “A Review of MEMS Capacitive Microphones,” *Micromachines*, vol. 11, no. 5, pp. 484, May 2020, Number: 5 Publisher: Multidisciplinary Digital Publishing Institute.
- [11] Knowles Electronics, “Knowles SPH0641LM4H-1 Datasheet (rev. D),” 2018.
- [12] Akustica, Inc., “AKU240 Family Datasheet 1.1a,” June 2016.
- [13] TDK InvenSense, “Microphone Specifications Explained, Application Note AN-1112, revision 1.1,” 2016.
- [14] Sorama, “Sorama CAM64 Specifications,” 2019.
- [15] Institute of Electrical and Electronics Engineers, “IEEE 1588-2008 - IEEE Standard for a Precision Clock Synchronization Protocol for Networked Measurement and Control Systems,” 2008.
- [16] Svend Gade and Henrik Herlufsen, “Technical Review: Windows to FFT Analysis (Part I),” 1987.
- [17] International Electrotechnical Commission, “IEC 60942, Electroacoustics - Sound calibrators,” 2017.
- [18] International Electrotechnical Commission, “IEC 61094-1/2/3/4/5/6/7/8, Measurement microphones, series of microphone and calibration standards,” 2016.
- [19] E. Frederiksen, “Acoustic metrology – an overview of calibration methods and their uncertainties,” *International Journal of Metrology and Quality Engineering*, vol. 4, no. 2, pp. 97–107, 2013, Number: 2 Publisher: EDP Sciences.
- [20] Andrea Prato, Nicola Montali, Claudio Guglielmo, and Alessandro Schiavi, “Pressure calibration of a digital microelectromechanical system microphone by comparison,” *The Journal of the Acoustical Society of America*, vol. 144, no. 4, pp. EL297–EL303, Oct. 2018, Publisher: Acoustical Society of America.
- [21] Randall P. Wagner and Steven E. Fick, “Pressure reciprocity calibration of a MEMS microphone,” *The Journal of the Acoustical Society of America*, vol. 142, no. 3, pp. EL251–EL257, Sept. 2017, Publisher: Acoustical Society of America.
- [22] Allan J. Zuckerwar, G. C. Herring, and Brian R. Elbing, “Calibration of the pressure sensitivity of microphones by a free-field method at frequencies up to 80kHz,” *The Journal of the Acoustical Society of America*, vol. 119, no. 1, pp. 320–329, Jan. 2006, Publisher: Acoustical Society of America.
- [23] Z. Havránek, P. Beneš, and S. Klusáček, “Free-field calibration of mems microphone array used for acoustic holography,” 2014, vol. 6, pp. 4513–4520.
- [24] Richard F. Potthoff, “Degrees of freedom,” in *Encyclopedia of Biostatistics*. American Cancer Society, 2005.